

1
2
3 FRONT MATTER
4

5 Melanopsin⁺RGCs are fully resistant to NMDA- 6 induced excitotoxicity.

7
8 **Running title:** m⁺RGCs Long-term effects of NMDA-induced excitotoxicity.
9

10 **AUTHOR LIST AND AFFILIATIONS:**

11
12 **Beatriz Vidal-Villegas^{*1}, Johnny Di Pierdomenico^{*1}, Juan A Miralles de Imperial-Ollero¹, Arturo**
13 **Ortín-Martínez^{1,3}, Francisco M Nadal-Nicolás^{1,4}, Jose M Bernal-Garro¹, Nicolás Cuenca Navarro²,**
14 **Maria P Villegas-Pérez¹, Manuel Vidal-Sanz^{**1}.**

15
16 ¹ Department of Ophthalmology, University of Murcia and Instituto Murciano de Investigación Biosanitaria
17 (IMIB)-Virgen de la Arrixaca, Murcia, Spain.

18 ² Department of Physiology, Genetics and Microbiology and Multidisciplinary Institute for Environmental
19 Studies "Ramón Margalef", University of Alicante, Alicante, Spain.

20 ³ Present address: Donald K Johnson Eye Institute, Krembil Research Institute, University Health Network,
21 Ontario, Canada.

22 ⁴ Present address: Retinal Neurophysiology Section, John Edward Porter Neuroscience Research Center,
23 National Eye Institute, National Institutes of Health, Bethesda, MD 20892, USA.
24

25 *Joint first authors

26 ** Correspondence: manuel.vidal@um.es
27
28
29

30 **Abstract**

31
32 We studied short- and long-term effects of intravitreal injection of N-methyl-D-aspartate (NMDA) on
33 melanopsin-containing (m⁺) and non-melanopsin-containing (Brn3a⁺) retinal ganglion cells (RGCs).
34 In adult SD-rats, the left eye received a single intravitreal injection of 5µL of 100nM NMDA. At 3 and
35 15 months, retinal thickness was measured *in vivo* using SD-OCT. Ex vivo analyses were done at 3,
36 7, 14 days or 15 months after damage. Whole-mounted retinas were immunolabelled for Brn3a and
37 melanopsin, the total number of Brn3a⁺RGCs and m⁺RGCs were quantified and their topography
38 represented. In control retinas, the mean total numbers of Brn3a⁺RGCs and m⁺RGCs were
39 78,903±3,572 and 2,358±144 (mean ± SD; n=10), respectively. In the NMDA injected retinas,
40 Brn3a⁺RGCs numbers diminished to 50% and 25%, at 3 and 14 days, respectively, but there was no
41 further loss up to 15 months. The number of immunoidentified m⁺RGCs decreased significantly at 3
42 days, recovered between 3-7 days and was back to normal thereafter. OCT measurements revealed a
43 significant thinning of the left retinas at 3 and 15 months. Intravitreal injections of NMDA induce a
44 rapid loss of 75% of Brn3a⁺RGCs, a transient downregulation of melanopsin expression but not
45 m⁺RGC death, and a thinning of the inner retinal layers.
46

47 **Key words**

48 NMDA, excitotoxicity, Glaucoma, melanopsin-RGCs, intrinsically photosensitive-RGCs,
49 Brn3a⁺RGCs, adult albino rat, retina, SD-OCT.
50
51

52 Research Manuscript Sections:

53

54 **Introduction**

55

56 Light is converted by photoreceptors (rods and cones) into electrical signals which are initially
57 processed at the outer synaptic layer of the retina where photoreceptor information is modulated by
58 horizontal cells and conveyed onto bipolar cells. Signals are further processed at the inner synaptic
59 layer where the bipolar information is modulated by amacrine cells and finally passed on to retinal
60 ganglion cells (RGCs) in the innermost retinal layer. RGCs, the only ones whose axon leaves the
61 retina, convey the information processed in the retina to the retinorecipient nuclei of the brain. This
62 projection obtains relevant information from our visual world from the retina and provides it to the
63 brain to produce image-forming as well as nonimage-forming visual functions. Retinal information
64 that produces image-forming visual functions is carried out by the general population of RGCs that
65 have in common the expression of Brn3a, while the information necessary to produce nonimage-
66 forming visual functions is carried out by a small subpopulation of RGCs that express the
67 photopigment melanopsin (m⁺RGCs) rendering them intrinsically photosensitive (ipRGCs); the so
68 called third photoreceptor cell-type of the retina [1].

69 In adult rodents, RGCs constitute less than 1% of all retinal cells [2-4]. Based on their morphology
70 (soma size and dendritic arborization), extension of their dendritic arborization into the inner synaptic
71 layer, electrophysiological responses to light stimulus within their receptive field, target region of the
72 brain and genetic background it has been proposed that the rodent retina may have up to 40 different
73 types of RGCs [5-8]. In the rat it has been estimated that excluding endothelial cells, the GCL is
74 composed of approximately 50% displaced amacrine cells (ACs), 10% glial cells, and 40% RGCs [9].
75 Displaced ACs not only share their location in the retina with RGCs but overlap in size thus making
76 it difficult to distinguish RGCs from ACs, and this has obliged the use of retrogradely transported
77 neuronal tracers [10,11] or neuronal markers to identify RGCs. There are several markers that identify
78 large proportions of RGCs (pan-markers) or many RGC types, including Thy-1 [12], Brn3a [13,14],
79 RBPMS [15], class III beta-tubulin [16], Neuronal Nuclei (NeuN) [17] and Microtubule-associated
80 protein 1A (MAP 1A) [7,18]. In addition, there are several markers that allow to identify specific types
81 of RGCs, such as melanopsin [19] and others [7,8,20]. However, after retinal injury, many of the
82 physiological and morphological attributes of RGCs, including their dendritic arborization may
83 change [8,21,22], and the molecular markers may be downregulated, rendering the identification of
84 RGCs difficult [23-28].

85 The characterization of the expression of Brn3a by rodent RGCs has allowed identification of the
86 main population of RGCs that convey image-forming visual information to the brain, which
87 represents approximately 96% of the RGC population [14]. Nonimage-forming visual behaviours
88 depend on intrinsically photosensitive RGCs (ipRGCs), one type of RGC with a large dendritic arbor
89 that contains the photopigment melanopsin (m⁺RGCs), responsible for the circadian
90 photoentrainment, pupillary reflexes and the regulation of pineal melatonin secretion [1,29,30]. Six
91 subtypes of ipRGCs have been described to express at least small amounts of melanopsin (also known
92 as Opn4), and are named M1-M6 [31,32]. Antibodies against melanopsin allow the identification of
93 the large majority of ipRGCs, preferentially M1-M3, because M4, which corresponds to the ON α RGC
94 subtype [33,34], M5 [35] and M6 [32] express less Opn4 than M1-M3 and are difficult to identify with
95 standard immunohistochemistry [31,32,36-39]. In rats, the population of m⁺RGCs constitute
96 approximately 2.5 and 2.7% of the RGC population for pigmented and albino, respectively [13,14,19].
97 Moreover, because Brn3a and melanopsin are hardly-ever expressed in the same RGC,
98 immunohistofluorescent studies using these two markers together allows the study, in parallel but
99 independently, of the responses of these two types of RGCs to different retinal injuries [28,40].

100 Glutamate excitotoxicity may be induced by the intravitreal injection of N-methyl D-Aspartate
101 (NMDA) which results in the excessive stimulation of NMDA receptors, one of the three ionotropic
102 glutamate receptor subtypes widely expressed by inner retinal neurons. Glutamate excitotoxicity is
103 thought to play an important role in the loss of RGCs in various retinal injuries [41,42] including
104 glaucoma [43-47], transient ischemia [48] and optic nerve injury [49,50], and may also play a key role

105 in many CNS diseases involving neuronal death [51]. Excessive NMDA receptor stimulation may
106 result in alterations of the Na⁺/K⁺ homeostasis, excessive influx of large amounts of Ca²⁺ into the cell
107 [52] which may result in direct damage by activation of enzymes that damage DNA and cell
108 membranes [53] and by the induction of apoptosis through activation of c-AMP [54]. Animal models
109 of NMDA-induced retinal excitotoxicity are often used to explore molecular mechanisms of RGC
110 apoptosis and its protection [55-63].

111 The susceptibility of RGCs to NMDA-mediated excitotoxicity has been studied previously in adult
112 rats [55,59] and mice [56,64], as well as the effects of intravitreal NMDA on the specific type
113 population of m⁺RGCs [56,64]. However, these were short term studies spanning up to 58 days after
114 NMDA injection and thus the short- and long-term effects of NMDA excitotoxicity on the population
115 of RGCs expressing Brn3a had not been investigated so far. Moreover, to what extent NMDA-
116 induced neurotoxicity may result in long term effects on the retinal architecture and on the
117 population of ipRGCs itself had not been previously investigated.

118 In the present studies we take advantage of recent techniques developed in the laboratory to
119 identify, count and map in the same retinal wholemounts the populations of RGCs expressing Brn3a
120 or melanopsin. Moreover, we use modern non-invasive techniques, such as the Spectral Domain
121 Optical Coherence Tomography (SD-OCT), to image and analyse retinal thickness longitudinally at
122 short (3months) and long (15 months) survival intervals. We investigate the responses of the general
123 population of RGCs (Brn3a⁺) and the population of ipRGCs (m⁺RGCs) to excitotoxicity induced by
124 the intravitreal injection of NMDA. Overall our studies indicate that the general population of
125 Brn3a⁺RGCs is quite sensible to NMDA mediated excitotoxicity and induces very rapidly the loss of
126 approximately 75% of the population. In contrast, m⁺RGCs after a transient downregulation of
127 melanopsin, show a remarkable capacity for survival of the entire m⁺RGC population, for periods of
128 up to 15 months. Examination of these retinas with SD-OCT reveals that NMDA-injected retinas
129 showed an important reduction in the thickness of the total and inner retina that was present at 3
130 months and progressed up to 15 months. Short accounts of this work have been published in abstract
131 format [65].

132

133 **Results**

134

135 We have included in this study a total of 51 rats whose left eye received an intraocular injection
136 of 5 µl NMDA (100nM). The first 28 were analysed within the first 14 days after the injection while
137 the remaining 23 were analysed at 15 months to investigate the long-term effects of the excitotoxic
138 insult on the survival of two RGC populations, the Brn3a⁺RGCs and the m⁺RGCs. Five additional
139 naïve rats were used as controls. In addition, SD-OCT was used to measure retinal thickness in both
140 retinas of each animal at 3 and 15 months after NMDA injection.

141

142 **Rapid and massive loss of Brn3a⁺RGCs shortly after NMDA injection.**

143 When the right and naïve retinas or the vehicle injected retinas, were examined under the
144 fluorescence microscope, Brn3a⁺RGCs showed the typical distribution throughout the entire retina
145 with higher densities on the superior retina, just above the optic nerve along the visual streak, as
146 described in detail before [66-68]. Changing the fluorescent filter allowed to see m⁺RGCs distributed
147 in a complementary fashion to Brn3a⁺RGCs and, as previously shown by this Laboratory [14,19], we
148 were not able to see any doubly immunolabelled RGC, thus confirming that these markers are
149 exclusive to one population (Figure 1).

150

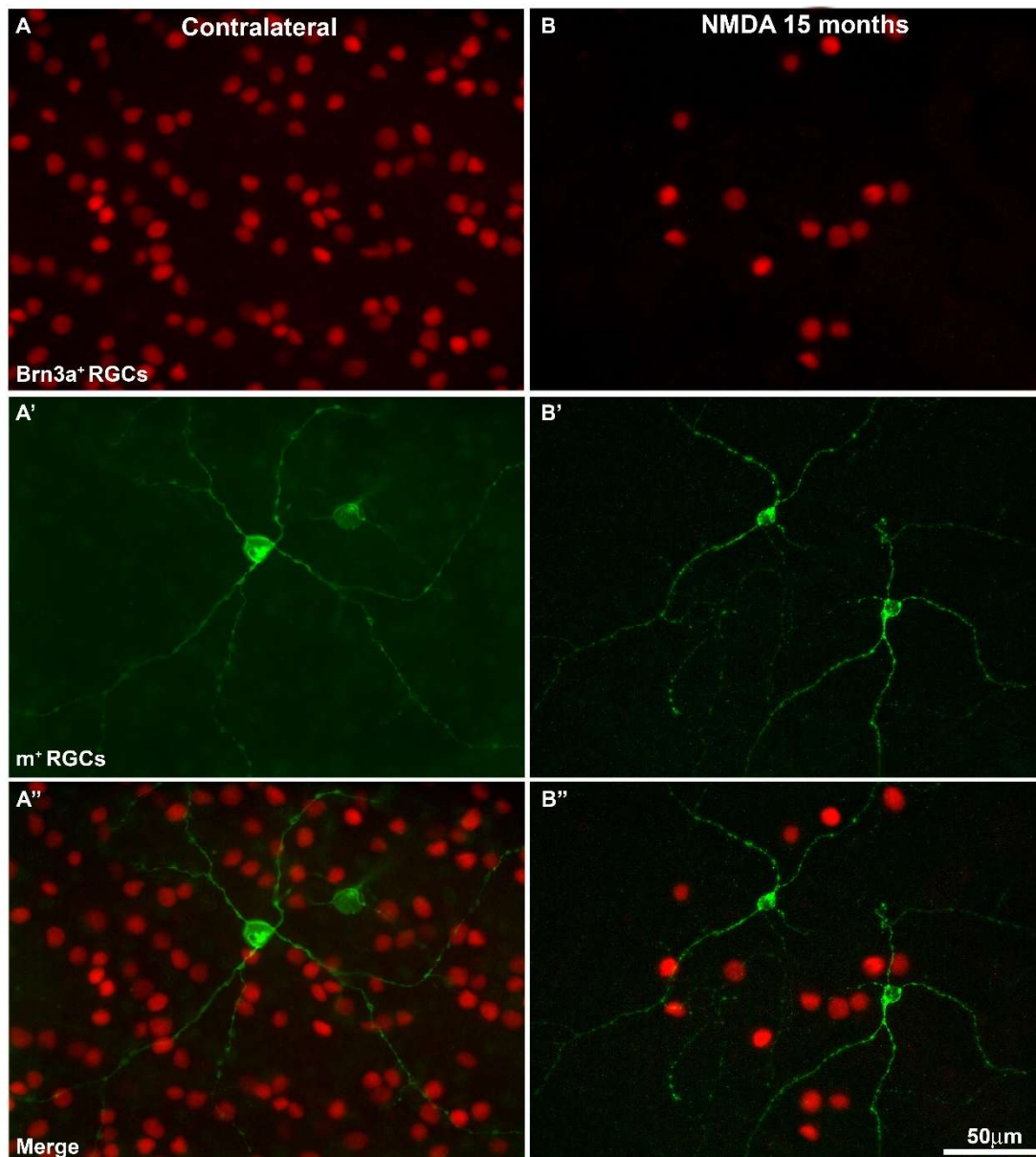


Figure 1. Magnifications from flat mounted retinas showing Brn3a⁺RGCs (A-B) and m⁺RGCs (A'-B') and both signals (merge) (A''-B'') in contralateral (A-A'') and NMDA-treated retinas (B-B'') analyzed at 15 months after the injection. Brn3a labels cell nuclei while melanopsin allows to see cell somata as well as primary dendrites on the plane of focus. When both images are overlapped (A''-B'') one can appreciate the smaller density of m⁺RGCs compared to Brn3a⁺RGCs, as well as the fact that there are no doubly labelled RGCs. Note that 15 months after NMDA injection there are fewer Brn3a⁺RGCs. Scale bar= 50 μ m.

151

152 Total numbers of Brn3a⁺RGCs (78,903 \pm 3,573 mean \pm SD, n=10) in the naïve retinas were
 153 comparable to those in the right fellow retinas of our experimental groups analysed at 3, 7 and 14
 154 days (76,472 \pm 5,815 Brn3a⁺RGCs mean \pm SD, n=29), or 15 months (81,480 \pm 5,602 mean \pm SD, n=20) after
 155 NMDA injection, as well as to those obtained in previous studies from this Laboratory [13,14,19,69]
 156 (Figures 1, 2. Table 1).

157 The left NMDA-injected retinas showed significant decreases in the total numbers of Brn3a⁺RGCs.
 158 By 3 days after NMDA injection, the total number of Brn3a⁺RGCs was 38,940 \pm 22,443 (n=9) which is
 159 significantly smaller than naïve controls and contralateral retinas ($p \leq 0.001$, Mann Whitney test).
 160 There were further reductions at 7 (21,811 \pm 9,750 mean \pm SD, n=6) and 14 days (19,348 \pm 8,502 mean \pm SD,
 161 n=10) but these were not statistically significant when compared to 3 days, indicating that in this
 162 injury model RGC loss occurs early after NMDA injection but there is no further progression between
 163 3 and 14 days (Figure 2, Table 1). Moreover, at 15 months, the left NMDA-injected retinas showed

164 significantly lower numbers than their fellow retinas ($15,099 \pm 8,595$ mean \pm SD, $n=23$) that
 165 corresponded to a survival of approximately 19%, although these values were not different from
 166 those obtained at 14 days (Mann Whitney test, $p=0,342$), indicating that there is no further loss of
 167 Brn3a⁺RGCs between 14 days and 15 months. (Figures 1, 2, 3, Table 1).
 168

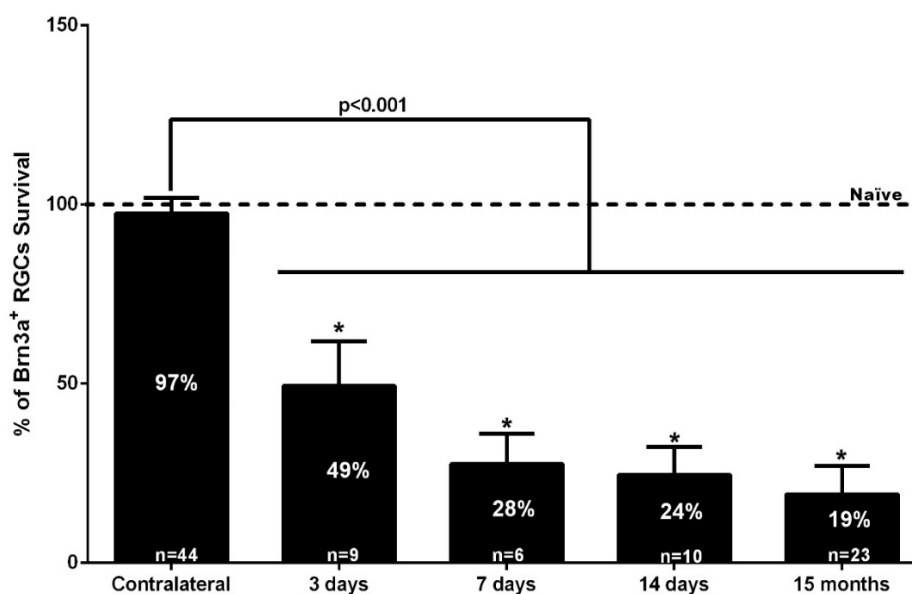


Figure 2. Bar graph showing the percent vs. intact retinas of the total numbers of Brn3a⁺RGCs \pm standard deviation quantified in the contralateral uninjured and experimental retinas analyzed 3, 7, 14 days (d) or 15 months (m) after the intraocular injection of 100 nM NMDA. The number of Brn3a⁺RGCs in the intact naïve retinas was considered 100%. The number of analyzed retinas is shown at the bottom of each bar. Statistically significant differences were observed (Kruskal-Wallis test, $p<0.001$) between values obtained in intact retinas (Naïve) or right eye retinas (Contralateral) and retinas examined at 3, 7, 14 days or 15 months. However, no significant differences were observed (*Kruskal-Wallis test, $p>0.05$) between experimental groups analyzed at 3, 7, 14 days or 15 months, which suggests that NMDA-induced Brn3a⁺RGCs does not progress between 3 days and 15 months.

169

170 Retinal distribution of Brn3a⁺RGCs in the NMDA injected retinas did not adopt any particular
 171 spatial pattern, their loss was diffuse and distributed over the entire retinas (Figure 3), although
 172 occasionally there was a smaller density in the superior temporal quadrant that could be explained
 173 by the proximity to the intraocular puncture and thus, a region exposed to a greater concentration of
 174 the injected NMDA.

175 **After a transient downregulation of melanopsin, m⁺RGCs appear fully resistant to NMDA**
 176 **injection.**

177 Total numbers of m⁺RGCs ($2,358 \pm 143$ mean \pm SD, $n=10$) in the naïve retinas were comparable to
 178 those obtained in the right fellow retinas of our experimental groups analysed at 3, 7 and 14 days
 179 ($2,257 \pm 228$ m⁺RGCs mean \pm SD, $n=29$), or at 15 months ($2,166 \pm 96$ mean \pm SD, $n=9$) after NMDA injection,
 180 as well as to those obtained in previous studies from this Laboratory [13,19,69] (Figures 1,3,4 Table
 181 2).

182

183 By 3 days after intravitreal injection of NMDA, the total number of m⁺RGCs was $1,516 \pm 312$ ($n=10$), a
 184 significant reduction when compared to naïve or contralateral retinas ($p \leq 0.001$, Kruskal Wallis test)
 185 (Figure 2). Surprisingly, the total number of m⁺RGCs at 7 or 14 days after NMDA injection was
 186 $2,105 \pm 445$ ($n=7$) or $2,419 \pm 257$ ($n=11$), showing a significant increase when compared to the values
 187 observed at 3 days, and reached comparable values to those of control retinas by 14 days ($p > 0.05$
 188 Kruskal Wallis, test). By 15 months after NMDA-injection, the left retinas showed a total number of
 189 m⁺RGCs ($2,027 \pm 134$ mean \pm SD, $n=11$) comparable with the data obtained in their right fellow retinas
 190 ($2,166 \pm 96$ mean \pm SD, $n=9$) (Mann Whitney test, $p=0.518$).

191

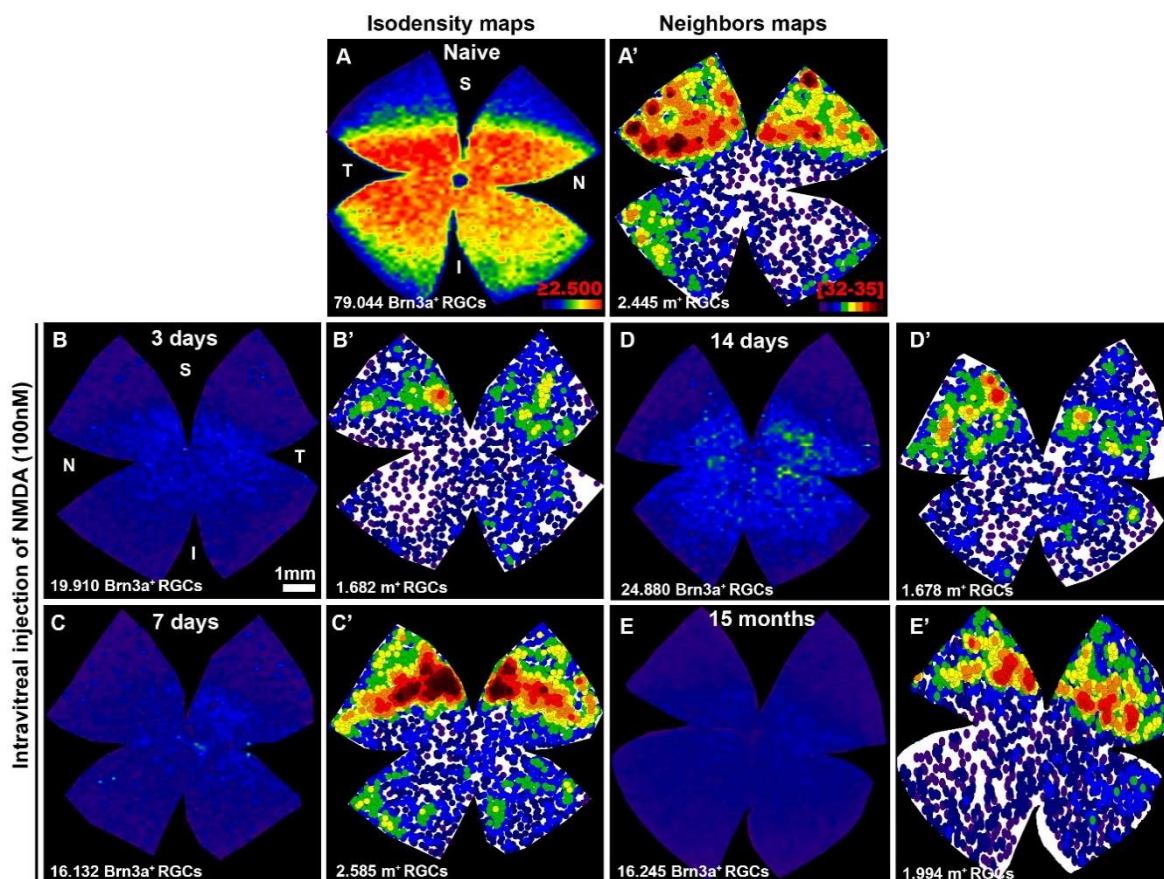


Figure 3. A-E. Isodensity maps showing the retinal topography of Brn3a⁺RGCs in intact retinas (A) or in representative retinas analyzed at 3 (B), 7 (C), 14 (D) days or 15 (E) months after intravitreal injection of 100nM NMDA. A'-E'. Neighbor maps illustrating the distribution of m⁺RGCs in the same retinas shown in A-E. Isodensity maps color scale ranges from 0 (purple) to ≥2,500 (red) cells/mm². Neighbor map color scale, each color represents an increase of 4 neighbors in a radius of 0.0552 mm from purple (0-4 neighbors) to dark red (32-35 neighbors). Below each map is shown the total number of Brn3a⁺RGCs or m⁺RGCs counted. S: superior, I: inferior, N: nasal, T: temporal. Scale bar= 1mm

192

193

194

195

196

197

198

199

200

201

In Vivo SD-OCT measurements

202

203

204

205

206

207

208

209

210

211

We interpret this abrupt decrease and subsequent recovery of the total number of m⁺RGCs as a transient downregulation of melanopsin, shortly after intravitreal injection of NMDA, that recovers up to normal levels of expression and total number of m⁺RGCs by 7, 14 days and 15 months. In addition, these results also indicate that m⁺RGCs are resistant to NMDA-induced excitotoxicity. In contrast with the Brn3a⁺RGC population, whose total numbers were reduced to approximately one quarter to one fifth of their normal values, the m⁺RGCs show a complete population that is comparable to that found in their fellow contralateral and in naïve retinas (Figures. 1,3,4, Table 2).

We wanted to examine the effects of the NMDA-induced retinal degeneration on the retinal layers and thus retinas were analysed at 3 and 15 months with SD-OCT to determine the total and inner retinal thickness. Figure 5 shows representative SD-OCT images from both eyes in two representative experimental rats analysed longitudinally *in vivo* 3 and 15 months after NMDA-injection. The SD-OCT provided measurements of the 31 sections acquired, and we selected three sections located superior, central or inferior for its analysis. Because the measurements of these three sections were comparable within each individual retina and time interval examined, the values from these 3 sections were pooled and used as a value for each retina and time point.

Total numbers of Brn3a ⁺ RGCs										
Retinas	Naïve		3 days		7 days		14 days		15 months	
	RE	LE	RE	LE	RE	LE	RE	LE	RE	LE
1	80293	82587	72071	46569	74963	24880	71159	16434	89717	14852
2	80399	79044	79209	52957	77604	12227	80940	13785	93939	9538
3	78344	71826	78178		72411	33105	78786	10593	88081	24936
4	74865	77395	79256	19910	66564		73895	39166	81353	21955
5	84031	80247	82406	15648	66086	31097	77579	16132	78436	22369
6			74244	15721	63952	9238	82321		68961	1951
7				62993	71202	20321	87289	15318	83471	5796
8				62344			80773	22261	80699	21478
9				61640			84397	20945		16245
10				12681			80789	12209		24937
11							76135	26641	74808	16594
12									88721	8588
13									75941	1990
14										2754
15									80213	10950
16									81595	5404
17									80424	5584
18									79487	25879
19									79093	25486
20									77667	21966
21									81417	11286
22									83543	25152
23									82032	21587
Mean	78903		77561	38940	70397	21811	79460	19348	81480	15099
± SD	3572		3757	22443	5038	9751	4631	8502	5602	8595
Total RE	Mean 78677 SD 6260									

Table 1. Total number of Brn3a⁺RGCs.

212

213

214

215

216

217

218

219

220

221

222

223

224

225

226

227

Total retinal (TR) thickness (as measured in μm from the inner side of the nerve fibre layer to the outer limit of the outer segment layer) was significantly smaller in the NMDA-injected retinas as compared to their contralateral fellow retinas at 3 (185 ± 4 versus 212 ± 3.2 ; $n=23$) and 15 (162 ± 6.1 versus 196 ± 6.1 ; $n=23$) months. In fact, the thinning of the TR was mainly due to the thinning of the inner retina (IR) (as measured in μm from the inner side of the nerve fibre layer to the outer limit of the inner nuclear layer). The IR thickness in the left NMDA-injected eyes was significantly smaller than in their fellow retinas at 3 (83 ± 3.7 versus 97 ± 4.2 ; $n=23$) and 15 (71 ± 2.8 versus 91 ± 3.4 ; $n=23$) months (Figures. 5,6).

The TR thickness of the fellow retinas diminished significantly between 3 (212 ± 3.2 ; $n=23$) and 15 (196 ± 6.1 ; $n=23$) months, a finding that is in agreement with recent studies in adult albino rats showing a physiological thinning of the TR and IR of approximately 16 and 6 μm , respectively, with age [69]. However, superimposed to the physiological age-related thinning of the retina, in the experimental NMDA-injected retinas there was further significant thinning of the TR (23 μm) and IR (12 μm) between 3 and 15 months (Figures. 5, 6).

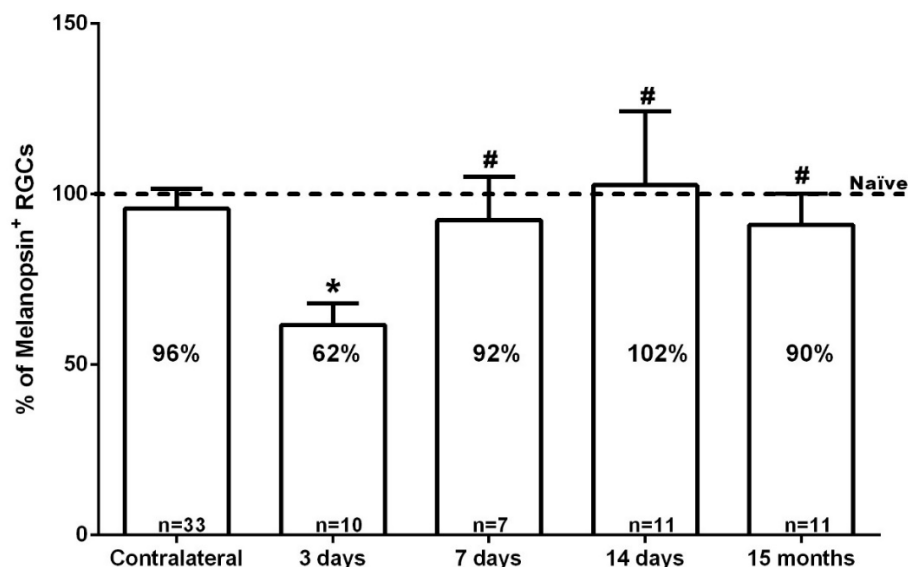


Figure 4. Bar graph showing the percent vs. intact retinas of the total number of m⁺RGCs ± standard deviation quantified in the contralateral uninjured and experimental retinas analyzed 3, 7, 14 days or 15 months after the intraocular injection of 100 nM NMDA. The number of analyzed retinas is shown at the bottom of each bar. *Significant differences compared to naïve, contralateral retinas and other timepoints (Kruskal-Wallis test, p<0.001). # The percent of m⁺RGCs in the experimental groups analyzed at 7d, 14 days or 15 months did not differ significantly from their contralateral fellow retinas (Mann-Whitney Test, p>0.05).

228

229

230 **Discussion**

231

232 Here we have investigated the short- and long-term responses of the populations of Brn3a⁺ and
 233 melanopsin expressing (m⁺) RGCs after an excitotoxic insult to the retina. Our studies show that
 234 following an intraocular injection of 100 nM NMDA, there is a rapid and massive loss of the general
 235 population of Brn3a⁺RGCs; by 3, 14 days or 15 months, the surviving population represents
 236 approximately 49%, 28% or 19%, respectively of the original population. When examined with SD-
 237 OCT there was an important reduction in the thickness of the total and the inner retina at 3 months
 238 that further progressed up to 15 months. Compared to the population of Brn3a⁺RGCs, m⁺RGCs show
 239 by 3 days a transient downregulation of melanopsin that recovers over the next weeks, and by 14
 240 days or 15 months the numbers of m⁺RGCs are comparable to their contralateral fellow eyes.

241 When studying the responses of RGCs to retinal injuries it is important to be able to identify
 242 different types of RGCs to understand how these respond to injury [40,70]. Here we use modern
 243 techniques developed in the Laboratory to count, image and represent the retinal topography of two
 244 RGC populations that can be readily identified with Brn3a and melanopsin [40,71]. Recent studies
 245 from this Laboratory have demonstrated that in the adult rat, retinal injuries induce a transient
 246 downregulation of melanopsin [28], followed by the expression of melanopsin in injured neurons
 247 surviving long periods of time [9,19,72,73]. Of the six main subtypes of ipRGCs M1-M6,
 248 immunocytochemistry against melanopsin identifies mainly M1-M3 because they show higher levels
 249 of melanopsin expression [32-35,37,38] and thus when interpreting our data, we should take into
 250 account that our immunohistochemical methods identify primarily the M1-M3 ipRGC subtypes. In
 251 fact, although not analysed in this work, it is conceivable that most of our results refer to the M1 and
 252 M2 subtypes which are the most abundant and readily identified with melanopsin antibodies
 253 [37,38,74].

254

Total numbers of melanopsin ⁺ RGCs										
Retinas	Naive		3 days		7 days		14 days		15 months	
	RE	LE	RE	LE	RE	LE	RE	LE	RE	LE
1	2434	2201	2135	2062	2163	1678	2034	2409		1994
2	2373	2445	1972	1293	2496	1650	2026	2276		2018
3	2366	2103	2294	1187	1962	1860	2055	2149	2154	1997
4	2362	2249	2547	1682	2262	1971	2242	2425	2297	1987
5	2612	2433	1966	1043	2040	2174	2566	2585	2207	1904
6			2183	1448	2471	2662	2363	2145	2016	1857
7				1719	2612	2746	1950	2661	2267	2019
8				1473			2537	2701	2022	2284
9				1850			2267	1955	2156	1961
10				1411			2559	2660	2196	2004
11							2467	2652	2181	2273
Mean	2358		2183	1453	2287	2106	2279	2420	2166	2027
± SD	144		219	371	247	446	235	257	95	133
Total RE	Mean 2257 SD 229									

Table 2. Total numbers of m⁺RGCs.

255

256

Intravitreal injection of NMDA induces Brn3a⁺RGC death

257

The loss of RGCs observed after the injection of NMDA in our studies is comparable to that found by others in mice [56,64] or rat [50,55,75] analysed at survival intervals ranging 3-58 days. We noticed certain inter-animal variability in the total number of surviving Brn3a⁺RGCs at 3 days after NMDA injection, that was also reported by others [55,64] and could be due to an individual animal susceptibility, or to the fact that RGC loss has not concluded by that time interval. Inter-animal variability following other types of retinal injuries, such as intraorbital optic nerve cut or crush, an insult that results in axotomy of the entire RGC population, have been shown [9,76]. Another possible explanation for the inter-animal variability could be the fact that intravitreal injections may suffer a small reflux of the injected volume rendering the concentration of NMDA not exactly equal for all eyes. We have not investigated shorter survival intervals than 3 days, after NMDA injection, but other studies have suggested that following NMDA injection RGC loss appears as early as 6 hours after injection [77]. It is currently thought that NMDA induced excitotoxicity results in activation of the NMDA receptor and this leads to a massive influx of Ca⁺⁺ that acts as a second messenger to activate pathways that lead to apoptotic neuronal death [78], although the exact signalling pathways involved in NMDA-induced RGC death are not completely understood [58].

272

273

Intravitreal injection of NMDA induces a progressive retinal thinning

274

RGC degeneration results in the loss of neural processes that extend into the inner synaptic layer where they contact cone-bipolar and amacrine cells of different types forming an extensive neuropil that makes up a substantial proportion of the inner synaptic layer's volume. Our results indicate that NMDA-induced retinal excitotoxicity results in a significant decrease of the total (TR) and inner (IR) retinal thickness. This thinning was already apparent in the left NMDA-injected experimental retinas by 3 months when compared to their fellow retinas. The retinal thinning may be explained because over 75% of the Brn3a⁺RGC population is missing and their dendrites have degenerated thus prompting a thinning of the IPL [75], but also because NMDA-excitotoxicity results in loss of amacrine cells, as shown with TUNEL and morphometric techniques in adult pigmented mice [82-84] and albino rats [75,85]. The thinning of the TR and IR observed in the fellow retinas between 3 and 15 months is consistent with the physiological thinning of the adult SD rat retina with age [69]. However, superimposed on this physiological thinning, in the experimental retinas there was a progressive thinning of the TR and IR between 3 and 15 months, indicating a continuing retinal

286

287 degeneration prolonged beyond the time of NMDA injection and the period of Brn3a⁺RGC loss which
 288 concluded by 3 days after the injection. A possible explanation for the progressive thinning of the IR
 289 could be the secondary amacrine cell loss that follows RGC death observed after NMDA-induced
 290 neurotoxicity. Indeed, approximately 72% of the RGC types in the mice retina are coupled to ACs
 291 [86] which may possibly facilitate secondary cell loss of calretinin, calbindin and choline
 292 acetyltransferase immunopositive ACs via gap junctions [84].
 293

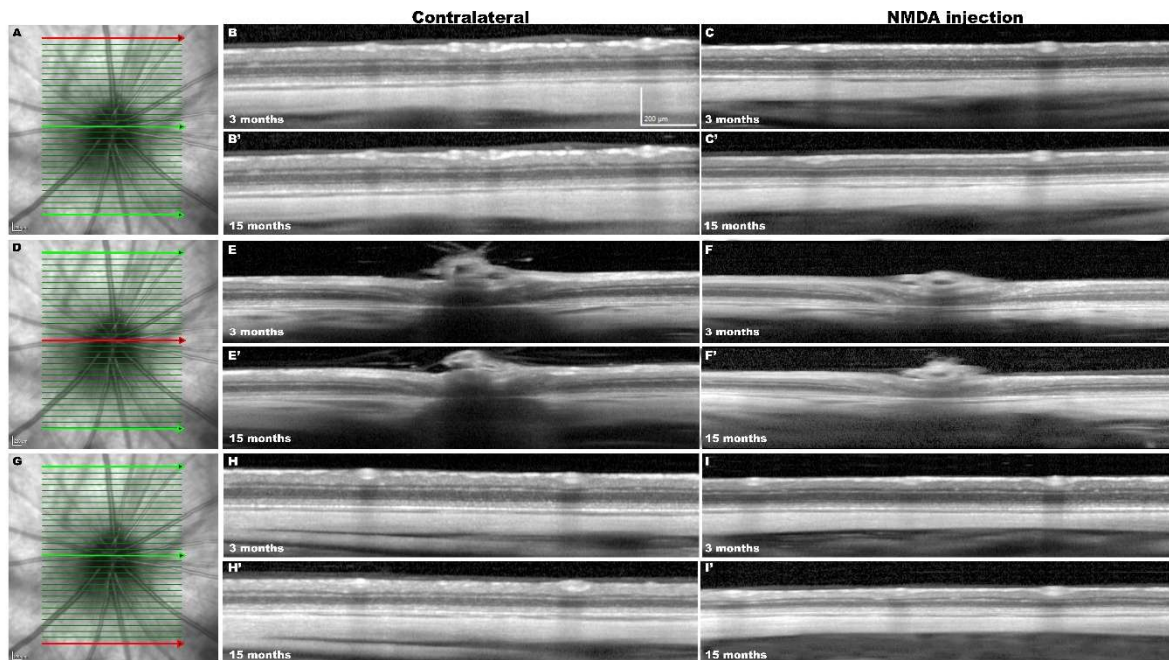


Figure 5. In vivo SD-OCT images from the same contralateral and experimental retinas analyzed 3 and 15 months after NMDA injection. (A, D, G) Representative images of the ocular fundus of the contralateral retina and position of the 31 sections acquired. The superior (A), central (D) or inferior (G) retinal sections are marked in red. (B, C, E, F, H, I) Representative sections acquired (in red) from SD-OCT volume raster scan in contralateral (B, E, H) and NMDA injected (C, F, I) retinas examined longitudinally at 3 (B-I) and at 15 (B'-I') months after NMDA injection

294
 295

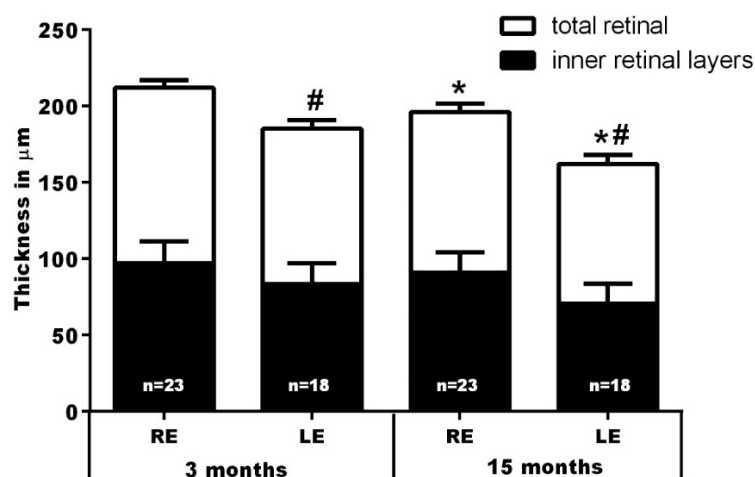


Figure 6. Graph bars showing the reduction of the mean \pm SD thickness (μm) of the total (from inner side of the nerve fibre layer to outer segment layer) and inner (from the inner side of the nerve fibre layer to outer margin of inner nuclear layer) retina after NMDA intravitreal injection into the left eye, measured in the volume scan analyses shown in Figure 5. *Significant differences compared to the same eyes analyzed at 3 months (One way Anova Kruskal-Wallis test, $p < 0.001$). # Significant differences when compared to their contralateral eyes at the same time interval (Mann-Whitney Rank Sum Test, $p < 0.001$). RE, right fellow eye. LE, left eye (NMDA-injected).

296 m⁺RGCs resilience to retinal disease and injury

297 In the adult rat m⁺RGCs only represent approximately 2,7% or 2,5% of the total population of
298 RGCs in albino or pigmented, respectively [14,19,69]. Yet, the availability of specific molecular
299 markers for this type of RGCs has made it possible to learn in a very short period of time a great deal
300 about the morphological and functional properties of these neurons, including their idiosyncratic
301 response to different types of inherited or acquired retinal lesions [40]. A number of different
302 laboratories have shown that ipRGCs demonstrate a much better survival against a variety of retinal
303 injuries than the general population of RGCs [87], and this particular resilience has been shown
304 against ocular hypertension in rats [39,88] or mice [89], optic nerve crush or cut in rats [90,91] or mice
305 [35,73,92,93], and transient ischemia of the retina in rats [81]. However, ipRGCs do not appear to be
306 particularly resilient in inherited models of retinal degeneration [94-96], mitochondrial optic
307 neuropathies [97] or degenerative diseases [74] such as Alzheimer [98], Parkinson [99] or Huntington
308 [100] disease [74]. A detailed characterization of the RGC responses to NMDA-induced excitotoxicity
309 may shed light into the paradigm of the different responses of different population of RGCs to injury;
310 why some populations die while others survive.

311

312 m⁺RGCs are resistant to NMDA-induced retinal excitotoxicity

313 Our results demonstrate that following a transient downregulation of melanopsin expression, the
314 total number of m⁺RGCs by 14 days or 15 months is comparable to their contralateral fellow eyes,
315 thus indicating an outstanding endurance to NMDA-induced excitotoxicity. Survival of the entire
316 m⁺RGC population by 15 months after NMDA injection is underscored in view of the important inner
317 retinal degeneration and loss of approximately 81% the Brn3a⁺RGC population. The degeneration of
318 RGCs following NMDA-induced excitotoxicity had been explored in adult pigmented mice analyzed
319 at 6 [64] or from 1 to 21 [56] days, respectively. However, these studies showed slight differences in
320 terms of the survival of the m⁺RGC population. DeParis and colleagues [64] found that 6 days after
321 NMDA injection there is a full component of m⁺RGC population surviving in the retina with no
322 downregulation of the expression of melanopsin, while Wang and colleagues [56] reported by 21
323 days after NMDA injection the loss of approximately one half of the m⁺RGC population. These
324 differences may be explained by the diverse amount of NMDA injected (3µl of 10 mM NMDA versus
325 1µl of 40 mM NMDA).

326 The downregulation of melanopsin expression that occurs after retinal injury requires further
327 consideration. Our studies reveal that following NMDA injection there is a transient downregulation
328 of melanopsin that recovers fully by 14 days. A similar transient downregulation of melanopsin has
329 been described in previous studies from this Laboratory in adult rats following optic nerve injury
330 [91], transient elevation of the intraocular pressure [81], the use of retrogradely transported neuronal
331 tracers [101] or acute light-induced retinal degeneration [72]. The differences between our results and
332 those observed by DeParis and colleagues [64] may be a species-specific response of m⁺RGCs, because
333 in parallel studies of m⁺RGCs survival in adult mice following intraorbital optic nerve injury we did
334 not find a transient downregulation of melanopsin [28,73].

335 Of all the retinal injuries examined so far, m⁺RGCs best afford NMDA-induced excitotoxicity. The
336 reasons for the remarkable resilience of ipRGCs to survive different types of injury-induced retinal
337 degeneration remain an open issue for future studies but several hypotheses have been forwarded to
338 explain m⁺RGCs resilience. One hypothesis proposes that these ipRGCs have large dendrites and
339 axon collaterals within the inner synaptic layer, and thus their intra-retinal connections may be
340 enough to provide trophic support for survival in the absence of brain target derived trophic support
341 [29,87,90,102]. Although it has been postulated that the absence of NMDA receptors in m⁺RGCs could
342 explain its particular resistance to NMDA mediated excitotoxicity, it has been shown that all RGCs
343 express NMDA receptor [103] including m⁺RGCs [63,104] and that the particular resilience of
344 m⁺RGCs is not related to pigmentation, genetic background, the presence of photoreceptors or the
345 activation of the endogenous survival JAK/STAT pathway [64]. Other possible explanations include
346 the activation of PI3K/AKT pathway after optic nerve cut or ocular hypertension [105], but this was
347 not apparent in NMDA-induced excitotoxicity [64]. Melanopsin itself could be thought to have an
348 effect on cell survival, but the fact that many ipRGCs survive with a transient, but lower, expression

349 of melanopsin makes this unlikely. Another hypothesis explains the resilience on the basis of their
350 neurotransmitter (PACAP) and it is hypothesized that PACAP would act as a neuroprotectant
351 conferring these neurons their particular resistance, since exogenous administration of PACAP
352 protects RGCs against optic nerve transection [106], ocular hypertension [107] or NMDA
353 administration [108]. It could also be possible that different types of RGCs may have different
354 responses to a same insult, thus arguing in favour of a type-specific susceptibility. For example, recent
355 studies using genetic markers to identify different types of RGCs have shown that the type of α RGCs
356 is particularly resistant to NMDA induced neurotoxicity [8] or to optic nerve crush [35,39], in contrast
357 to the very low survival of Junction adhesion molecules B expressing RGCs (J-RGCs) [8]. Moreover,
358 recent studies indicate that among subtypes of ipRGCs there are different susceptibility to specific
359 insults; for instance, in a mouse model of Huntington's disease (HD), M1 were reduced compared to
360 non-M1 ipRGCs which survived to HD progression [109]. Furthermore, in a mouse model of ocular
361 hypertension subtypes of α RGCs were found to have different susceptibility, with OFF-transient
362 α RGCs being more vulnerable than ON- or OFF-sustained α RGCs [22,70]. Overall, the particular
363 resilience of mRGCs makes them a suitable candidate to study changes in protein expression after
364 injury to further our knowledge about what makes a neuron survive better than others, and this
365 would in turn result in the design of new neuroprotective strategies for RGCs against noxious stimuli.
366 Thus, future studies are needed to decipher the molecular correlates that provide these neurons with
367 a self-built neuroprotection against various types of injury, including NMDA-induced RGC death.

368

369 **Material and Methods**

370

371 **Animal handling and experimental groups**

372 Experiments were prepared in 56 adult female SD rats (250g) obtained from the animal house (Murcia
373 University) and treated according to the European Union guidelines for Animal Care and use of
374 scientific purpose (Directive 2010/63/UE). All procedures were approved by the Ethical and Animal
375 Studies Committee of the University of Murcia, Spain. Animals had free access to food and water
376 and kept in a temperature and light controlled room with 12-hr/12-hr light/dark cycles. Animals were
377 anaesthetized with a mixture of xylazine (10mg/kg Rompun; Bayer, Kiel, Germany) and ketamine (60
378 mg/Kg bw, Ketolar; Pfizer, Alcobendas, Madrid, Spain). 0.5% proparacaine hydrochloride eye drops
379 (Alcon Co., Fort Worth, TX, USA) were used to achieve topical anaesthesia. After the surgical
380 procedures, an ocular ointment was placed over the corneas of both eyes to prevent corneal
381 desiccation (Tobrex®; Alcon-Cusí, S.A., Barcelona, Spain). Animals were divided into experimental
382 and control groups. The experimental group received an intraocular injection of NMDA and was
383 divided into four subgroups that were examined at 3 (n=10), 7 (n=7) or 14 (n=11) days, or 15 months
384 (n=23). Additional naïve rats (n=5) were used as controls. For animal sacrifice an overdose of sodium
385 pentobarbital injected intraperitoneally (Dolethal, Vetoquinol®, Especialidades Veterinarias, S.A.,
386 Madrid, Spain).

387

388 **Intraocular injections of NMDA**

389 Retinal excitotoxicity was induced in the left eye of the experimental animals by intraocular injection
390 of 5 μ l of 100nM NMDA N-methyl-D-Aspartate (NMDA) (M3262; Sigma-Aldrich Química S.A.,
391 Madrid, Spain) dissolved in 0.1 M phosphate buffer saline (PBS) following standard techniques in
392 our Lab [110-112]. In brief, a small puncture in the sclera approximately 1 mm from the limbus was
393 made with a 30-gauge needle, and then NMDA was injected slowly with a Hamilton syringe whose
394 needle was introduced through the sclerotomy. After injection, the needle was withdrawn slowly
395 and an ointment (Tobrex pomada; Alcon S.A., Barcelona, Spain) was placed over the eyes to prevent
396 corneal dehydration until anaesthesia recovery. The contralateral non-injected eye was used as
397 control, 5 naïve rats (10 eyes) were also used as controls. Preliminary experiments (data not shown)
398 allowed us to try increasing doses of NMDA to find one that would result in consistent RGC death.
399 Previous studies from this Laboratory did not find any effect of the intraocular injection of vehicle
400 alone (0.1 M phosphate buffer saline, PBS) on the survival of the Brn3a⁺ or melanopsin⁺ RGC

401 populations (unpublished observations), and thus, we did not employ additional animals for this
402 purpose.

403

404 **In vivo measurements of the retinal thickness with SD-OCT**

405 SD-OCT measurements were obtained to analyse changes in the thickness of the retina following
406 NMDA intraocular injection, and the eyes were imaged at 3 and 15 months, as previously described
407 in detail [69,113]. Rats were anaesthetized systemically, and eye drops were placed on both eyes to
408 induce mydriasis (Tropicamide 1%; Alcon-Cusí, S.A.) and to prevent corneal desiccation (artificial
409 tears). Rats were placed in prone position over a platform with their heads upright and turned to the
410 opposite side of the inspected eye. The head position was kept similar for all animals and, and for the
411 following examination the follow up tool of the OCT program was used to compare the same regions.
412 A custom-made permeable contact lens (3.5-mm posterior radius of curvature, 5.0-mm optical zone
413 diameter, 5.0-diopter [D] back vertex power) was placed on the cornea to maintain hydration and
414 thus clarity. Both retinas were imaged using SD-OCT according to the manufacturer instructions
415 (Spectralis; Heidelberg Engineering, Heidelberg, Germany). To adapt for the rat's eye, a
416 commercially available 78-D double aspheric fundus lens (Volk Optical, Inc., Mentor, OH, USA) was
417 mounted in front of the camera unit. Imaging was performed with a software package (EyeExplorer,
418 version 3.2.1.0; Heidelberg Engineering). Retinal thickness was measured using a scanning pattern
419 centred on the optic nerve head; a raster scan of 31 equally spaced horizontal B-scans (3000 μm
420 length). For each section total retinal (TR) (as measured from the inner limiting membrane to the
421 outer limit of the pigmented epithelial layer) and inner retinal (IR) (as measured from the inner
422 limiting membrane to the outer limit of the inner nuclear layer) thickness were measured at distances
423 of 1800 μm from optic disc.

424

425 **Retinal dissection, immunohistochemistry and image acquisition**

426 At different survival intervals, rats were sacrificed and perfused through the heart, first and briefly
427 with a solution of 0.9% ClNa and then slowly with a 4% paraformaldehyde solution in PBS. The
428 superior pole of the eye was marked with a small suture, and retinas were then dissected and
429 prepared as flattened wholemounts as previously described [114]. Retinas were double-
430 immunodetected following previously described methods for Brn3a and melanopsin to identify
431 surviving RGCS expressing these two markers [14]. Primary antibodies were goat anti-Brn3a (1:750
432 dilution, C-20 Santa Cruz Biothecology, Heidelberg, Germany) and rabbit anti melanopsin (1:500
433 dilution, PAI-780, Invitrogen, Thermo Fisher Scientific, Alcobendas, Madrid, Spain). Secondary
434 antibodies were Alexa Fluor conjugated (donkey anti-rabbit Alexa 594, donkey anti-goat Alexa 488)
435 (Molecular Probes Thermo-Fisher, Madrid, Spain). After immunodetection retinas were mounted on
436 subbed slides with the vitreal side up and covered with antifading solution [14].

437

438 Photographic reconstructions of flattened whole-mount retinas were obtained under an
439 epifluorescence microscope (Axioscop 2 Plus; Zeiss Mikroskopie, Jena, Germany) equipped with a
440 computer driven motorized stage (ProScan H128 Series; Prior Scientific Instruments, Cambridge,
441 UK) according to previously described methods that are standard in the Lab [73,115]. A total of 154
442 frames were obtained in the microscope to reconstruct the whole retina. These reconstructions were
443 obtained under both filters to allow identification of Brn3a⁺RGCS and m⁺RGCS, respectively.
444 Following standard procedures in the Lab [71,116,117], wholemount reconstructions were further
445 processed to obtain automatically the total number of Brn3a⁺RGCS and their topographical
446 distribution was represented as isodensity maps. For the m⁺RGCS, these were quantified manually
447 and dotted on the photomontage with the aid of a graphic editing software Adobe Photoshop CS8.01
448 (Adobe Systems, Inc., San Jose, CA, USA). Dots were automatically identified, and their
449 topographical distribution represented as neighbour maps following previously described methods
450 [117].

451

452 **Statistics**

453 All data is expressed as means \pm standard deviation (SD). Statistical analysis employed the program
454 GraphPad Prism® for windows (Version 5.01; GraphPad Software Inc., La Jolla, CA, EEUU) using
455 non-parametric tests (Kruskal Wallis and Mann Whitney). Differences were considered significant if
456 $p < 0.05$.

457

458 **Conclusions**

459

460 Intravitreally administered NMDA in adult albino rats: i) induces a massive diffuse loss of
461 Brn3⁺RGCs already at 3 days that does not progress further; ii) Causes a thinning of the inner retina
462 by 3 months that further progresses up to 15 months; iii) Triggers a transient downregulation of
463 melanopsin expression, that is evident at 3 days and recovers fully by 14 days, and; iv) Does not
464 induce m⁺RGCs loss.

465

466 **Back Matter**

467

468 Supplementary materials

469 None

470

471 Acknowledgements

472 This study was supported by the Fundación Séneca, Agencia de Ciencia y Tecnología Región de
473 Murcia (19881/GERM/15), and the Spanish Ministry of Economy and Competitiveness, Instituto de
474 Salud Carlos III, Fondo Europeo de Desarrollo Regional “una manera de hacer Europa” (SAF2015-
475 67643-P, PI16/00380, RD16/0008/0026 and RD16/0008/0016).

476

477 Author Contributions

478 BVV, JDP, MVS and NC conceptualized the study. BVV, JDP, FMNN, JAMO, AOM, JMBG, NC,
479 MPVP, and MVS planned and performed all experiments and analysed data. JAMO and AOM
480 performed preliminary experiments to set up the model. JMBG analysed retinas and performed
481 image analysis for RGC counts. BVV, JDP, NC and MVS wrote the paper with input from all authors.
482 MPVP, MVS provided research funds for the study.

483

484 Conflicts of Interests

485 None

486

487 **References**

488

489 1. Lucas, R.J.; Peirson, S.N.; Berson, D.M.; Brown, T.M.; Cooper, H.M.; Czeisler, C.A.; Figueiro,

490 M.G.; Gamlin, P.D.; Lockley, S.W.; O'Hagan, J.B., et al. Measuring and using light in the

491 melanopsin age. *Trends in neurosciences* **2014**, *37*, 1-9, doi:10.1016/j.tins.2013.10.004.

492 2. Smith, C.A.; Chauhan, B.C. Imaging retinal ganglion cells: enabling experimental

493 technology for clinical application. *Progress in retinal and eye research* **2015**, *44*, 1-14,

494 doi:10.1016/j.preteyeres.2014.10.003.

495 3. Masland, R.H. The neuronal organization of the retina. *Neuron* **2012**, *76*, 266-280,

496 doi:10.1016/j.neuron.2012.10.002.

497 4. Macosko, E.Z.; Basu, A.; Satija, R.; Nemesh, J.; Shekhar, K.; Goldman, M.; Tirosh, I.; Bialas,

498 A.R.; Kamitaki, N.; Martersteck, E.M., et al. Highly Parallel Genome-wide Expression

499 Profiling of Individual Cells Using Nanoliter Droplets. *Cell* **2015**, *161*, 1202-1214,

500 doi:10.1016/j.cell.2015.05.002.

501 5. Baden, T.; Berens, P.; Franke, K.; Roman Roson, M.; Bethge, M.; Euler, T. The functional

502 diversity of retinal ganglion cells in the mouse. *Nature* **2016**, *529*, 345-350,

503 doi:10.1038/nature16468.

504 6. Sanes, J.R.; Masland, R.H. The types of retinal ganglion cells: current status and

505 implications for neuronal classification. *Annual review of neuroscience* **2015**, *38*, 221-246,

506 doi:10.1146/annurev-neuro-071714-034120.

507 7. Rheume, B.A.; Jereen, A.; Bolisetty, M.; Sajid, M.S.; Yang, Y.; Renna, K.; Sun, L.; Robson, P.;

508 Trakhtenberg, E.F. Single cell transcriptome profiling of retinal ganglion cells identifies

509 cellular subtypes. *Nature communications* **2018**, *9*, 2759, doi:10.1038/s41467-018-05134-3.

510 8. Christensen, I.; Lu, B.; Yang, N.; Huang, K.; Wang, P.; Tian, N. The Susceptibility of Retinal

511 Ganglion Cells to Glutamatergic Excitotoxicity Is Type-Specific. *Frontiers in neuroscience*512 **2019**, *13*, 219, doi:10.3389/fnins.2019.00219.

513 9. Nadal-Nicolas, F.M.; Salinas-Navarro, M.; Vidal-Sanz, M.; Agudo-Barriuso, M. Two

514 methods to trace retinal ganglion cells with fluorogold: from the intact optic nerve or by

515 stereotactic injection into the optic tract. *Experimental eye research* **2015**, *131*, 12-19,

516 doi:10.1016/j.exer.2014.12.005.

517 10. Thanos, S.; Vidal-Sanz, M.; Aguayo, A.J. The use of rhodamine-B-isothiocyanate (RITC) as

518 an anterograde and retrograde tracer in the adult rat visual system. *Brain research* **1987**, *406*,

519 317-321.

520 11. Vidal-Sanz, M.; Bray, G.M.; Villegas-Perez, M.P.; Thanos, S.; Aguayo, A.J. Axonal

521 regeneration and synapse formation in the superior colliculus by retinal ganglion cells in

522 the adult rat. *The Journal of neuroscience : the official journal of the Society for Neuroscience* **1987**,523 *7*, 2894-2909.

524 12. Barnstable, C.J.; Drager, U.C. Thy-1 antigen: a ganglion cell specific marker in rodent retina.

525 *Neuroscience* **1984**, *11*, 847-855.

526 13. Nadal-Nicolas, F.M.; Jimenez-Lopez, M.; Salinas-Navarro, M.; Sobrado-Calvo, P.;

527 Alburquerque-Bejar, J.J.; Vidal-Sanz, M.; Agudo-Barriuso, M. Whole number, distribution

528 and co-expression of brn3 transcription factors in retinal ganglion cells of adult albino and

529 pigmented rats. *PloS one* **2012**, *7*, e49830, doi:10.1371/journal.pone.0049830.

530 14. Nadal-Nicolas, F.M.; Salinas-Navarro, M.; Jimenez-Lopez, M.; Sobrado-Calvo, P.; Villegas-

531 Perez, M.P.; Vidal-Sanz, M.; Agudo-Barriuso, M. Displaced retinal ganglion cells in albino

532 and pigmented rats. *Frontiers in neuroanatomy* **2014**, *8*, 99, doi:10.3389/fnana.2014.00099.

533 15. Rodriguez, A.R.; de Sevilla Muller, L.P.; Brecha, N.C. The RNA binding protein RBPMS is a

534 selective marker of ganglion cells in the mammalian retina. *The Journal of comparative*535 *neurology* **2014**, *522*, 1411-1443, doi:10.1002/cne.23521.

- 536 16. Jiang, S.M.; Zeng, L.P.; Zeng, J.H.; Tang, L.; Chen, X.M.; Wei, X. beta-III-Tubulin: a reliable
537 marker for retinal ganglion cell labeling in experimental models of glaucoma. *International*
538 *journal of ophthalmology* **2015**, *8*, 643-652, doi:10.3980/j.issn.2222-3959.2015.04.01.
- 539 17. Dijk, F.; Bergen, A.A.; Kamphuis, W. GAP-43 expression is upregulated in retinal ganglion
540 cells after ischemia/reperfusion-induced damage. *Experimental eye research* **2007**, *84*, 858-867,
541 doi:10.1016/j.exer.2007.01.006.
- 542 18. McKerracher, L.; Vallee, R.B.; Aguayo, A.J. Microtubule-associated protein 1A (MAP 1A) is
543 a ganglion cell marker in adult rat retina. *Visual neuroscience* **1989**, *2*, 349-356.
- 544 19. Galindo-Romero, C.; Jimenez-Lopez, M.; Garcia-Ayuso, D.; Salinas-Navarro, M.; Nadal-
545 Nicolas, F.M.; Agudo-Barriuso, M.; Villegas-Perez, M.P.; Aviles-Trigueros, M.; Vidal-Sanz,
546 M. Number and spatial distribution of intrinsically photosensitive retinal ganglion cells in
547 the adult albino rat. *Experimental eye research* **2013**, *108*, 84-93, doi:10.1016/j.exer.2012.12.010.
- 548 20. Kim, I.J.; Zhang, Y.; Yamagata, M.; Meister, M.; Sanes, J.R. Molecular identification of a
549 retinal cell type that responds to upward motion. *Nature* **2008**, *452*, 478-482,
550 doi:10.1038/nature06739.
- 551 21. Agostinone, J.; Di Polo, A. Retinal ganglion cell dendrite pathology and synapse loss:
552 Implications for glaucoma. *Progress in brain research* **2015**, *220*, 199-216,
553 doi:10.1016/bs.pbr.2015.04.012.
- 554 22. Ou, Y.; Jo, R.E.; Ullian, E.M.; Wong, R.O.; Della Santina, L. Selective Vulnerability of
555 Specific Retinal Ganglion Cell Types and Synapses after Transient Ocular Hypertension.
556 *The Journal of neuroscience : the official journal of the Society for Neuroscience* **2016**, *36*, 9240-
557 9252, doi:10.1523/JNEUROSCI.0940-16.2016.
- 558 23. Chidlow, G.; Casson, R.; Sobrado-Calvo, P.; Vidal-Sanz, M.; Osborne, N.N. Measurement of
559 retinal injury in the rat after optic nerve transection: an RT-PCR study. *Molecular vision*
560 **2005**, *11*, 387-396.
- 561 24. Lonngren, U.; Napankangas, U.; Lafuente, M.; Mayor, S.; Lindqvist, N.; Vidal-Sanz, M.;
562 Hallbook, F. The growth factor response in ischemic rat retina and superior colliculus after
563 brimonidine pre-treatment. *Brain research bulletin* **2006**, *71*, 208-218,
564 doi:10.1016/j.brainresbull.2006.09.005.
- 565 25. Agudo, M.; Perez-Marin, M.C.; Lonngren, U.; Sobrado, P.; Conesa, A.; Canovas, I.; Salinas-
566 Navarro, M.; Miralles-Imperial, J.; Hallbook, F.; Vidal-Sanz, M. Time course profiling of the
567 retinal transcriptome after optic nerve transection and optic nerve crush. *Molecular vision*
568 **2008**, *14*, 1050-1063.
- 569 26. Agudo, M.; Perez-Marin, M.C.; Sobrado-Calvo, P.; Lonngren, U.; Salinas-Navarro, M.;
570 Canovas, I.; Nadal-Nicolas, F.M.; Miralles-Imperial, J.; Hallbook, F.; Vidal-Sanz, M.
571 Immediate upregulation of proteins belonging to different branches of the apoptotic
572 cascade in the retina after optic nerve transection and optic nerve crush. *Investigative*
573 *ophthalmology & visual science* **2009**, *50*, 424-431, doi:10.1167/iovs.08-2404.
- 574 27. Agudo-Barriuso, M.; Lahoz, A.; Nadal-Nicolas, F.M.; Sobrado-Calvo, P.; Piquer-Gil, M.;
575 Diaz-Llopis, M.; Vidal-Sanz, M.; Mullor, J.L. Metabolomic changes in the rat retina after
576 optic nerve crush. *Investigative ophthalmology & visual science* **2013**, *54*, 4249-4259,
577 doi:10.1167/iovs.12-11451.
- 578 28. Agudo-Barriuso, M.; Nadal-Nicolas, F.M.; Madeira, M.H.; Rovere, G.; Vidal-Villegas, B.;
579 Vidal-Sanz, M. Melanopsin expression is an indicator of the well-being of melanopsin-
580 expressing retinal ganglion cells but not of their viability. *Neural regeneration research* **2016**,
581 *11*, 1243-1244, doi:10.4103/1673-5374.189182.
- 582 29. Vugler, A.; Semo, M.; Ortin-Martinez, A.; Rojanasakul, A.; Nommiste, B.; Valiente-Soriano,
583 F.J.; Garcia-Ayuso, D.; Coffey, P.; Vidal-Sanz, M.; Gias, C. A role for the outer retina in

- 584 development of the intrinsic pupillary light reflex in mice. *Neuroscience* **2015**, *286*, 60-78,
585 doi:10.1016/j.neuroscience.2014.11.044.
- 586 30. Hannibal, J.; Christiansen, A.T.; Heegaard, S.; Fahrenkrug, J.; Kiilgaard, J.F. Melanopsin
587 expressing human retinal ganglion cells: Subtypes, distribution, and intraretinal
588 connectivity. *The Journal of comparative neurology* **2017**, *525*, 1934-1961, doi:10.1002/cne.24181.
- 589 31. Berson, D.M.; Castrucci, A.M.; Provencio, I. Morphology and mosaics of melanopsin-
590 expressing retinal ganglion cell types in mice. *The Journal of comparative neurology* **2010**, *518*,
591 2405-2422, doi:10.1002/cne.22381.
- 592 32. Quattrochi, L.E.; Stabio, M.E.; Kim, I.; Ilardi, M.C.; Michelle Fogerson, P.; Leyrer, M.L.;
593 Berson, D.M. The M6 cell: A small-field bistratified photosensitive retinal ganglion cell. *The*
594 *Journal of comparative neurology* **2019**, *527*, 297-311, doi:10.1002/cne.24556.
- 595 33. Sonoda, T.; Lee, S.K.; Bimbaumer, L.; Schmidt, T.M. Melanopsin Phototransduction Is
596 Repurposed by ipRGC Subtypes to Shape the Function of Distinct Visual Circuits. *Neuron*
597 **2018**, *99*, 754-767 e754, doi:10.1016/j.neuron.2018.06.032.
- 598 34. Estevez, M.E.; Fogerson, P.M.; Ilardi, M.C.; Borghuis, B.G.; Chan, E.; Weng, S.; Auferkorte,
599 O.N.; Demb, J.B.; Berson, D.M. Form and function of the M4 cell, an intrinsically
600 photosensitive retinal ganglion cell type contributing to geniculocortical vision. *The Journal*
601 *of neuroscience : the official journal of the Society for Neuroscience* **2012**, *32*, 13608-13620,
602 doi:10.1523/JNEUROSCI.1422-12.2012.
- 603 35. Duan, X.; Qiao, M.; Bei, F.; Kim, I.J.; He, Z.; Sanes, J.R. Subtype-specific regeneration of
604 retinal ganglion cells following axotomy: effects of osteopontin and mTOR signaling.
605 *Neuron* **2015**, *85*, 1244-1256, doi:10.1016/j.neuron.2015.02.017.
- 606 36. Berry, M.; Ahmed, Z.; Logan, A. Return of function after CNS axon regeneration: Lessons
607 from injury-responsive intrinsically photosensitive and alpha retinal ganglion cells. *Progress*
608 *in retinal and eye research* **2018**, 10.1016/j.preteyeres.2018.11.006,
609 doi:10.1016/j.preteyeres.2018.11.006.
- 610 37. Schmidt, T.M.; Chen, S.K.; Hattar, S. Intrinsically photosensitive retinal ganglion cells:
611 many subtypes, diverse functions. *Trends in neurosciences* **2011**, *34*, 572-580,
612 doi:10.1016/j.tins.2011.07.001.
- 613 38. Schmidt, T.M.; Do, M.T.; Dacey, D.; Lucas, R.; Hattar, S.; Matynia, A. Melanopsin-positive
614 intrinsically photosensitive retinal ganglion cells: from form to function. *The Journal of*
615 *neuroscience : the official journal of the Society for Neuroscience* **2011**, *31*, 16094-16101,
616 doi:10.1523/JNEUROSCI.4132-11.2011.
- 617 39. Li, S.; Yang, C.; Zhang, L.; Gao, X.; Wang, X.; Liu, W.; Wang, Y.; Jiang, S.; Wong, Y.H.;
618 Zhang, Y., et al. Promoting axon regeneration in the adult CNS by modulation of the
619 melanopsin/GPCR signaling. *Proceedings of the National Academy of Sciences of the United*
620 *States of America* **2016**, *113*, 1937-1942, doi:10.1073/pnas.1523645113.
- 621 40. Vidal-Sanz, M.; Nadal-Nicolas, F.M.; Valiente-Soriano, F.J.; Agudo-Barriuso, M.; Villegas-
622 Perez, M.P. Identifying specific RGC types may shed light on their idiosyncratic responses
623 to neuroprotection. *Neural regeneration research* **2015**, *10*, 1228-1230, doi:10.4103/1673-
624 5374.162751.
- 625 41. Lucas, D.R.; Newhouse, J.P. The toxic effect of sodium L-glutamate on the inner layers of
626 the retina. *A.M.A. archives of ophthalmology* **1957**, *58*, 193-201.
- 627 42. Choi, D.W. Glutamate neurotoxicity and diseases of the nervous system. *Neuron* **1988**, *1*,
628 623-634.
- 629 43. Dreyer, E.B.; Zurakowski, D.; Schumer, R.A.; Podos, S.M.; Lipton, S.A. Elevated glutamate
630 levels in the vitreous body of humans and monkeys with glaucoma. *Arch Ophthalmol* **1996**,
631 *114*, 299-305.

- 632 44. Izzotti, A.; Bagnis, A.; Sacca, S.C. The role of oxidative stress in glaucoma. *Mutation research*
633 2006, 612, 105-114, doi:10.1016/j.mrrev.2005.11.001.
- 634 45. Tezel, G. Immune regulation toward immunomodulation for neuroprotection in glaucoma.
635 *Current opinion in pharmacology* 2013, 13, 23-31, doi:10.1016/j.coph.2012.09.013.
- 636 46. Vorwerk, C.K.; Kreutz, M.R.; Bockers, T.M.; Brosz, M.; Dreyer, E.B.; Sabel, B.A.
637 Susceptibility of retinal ganglion cells to excitotoxicity depends on soma size and retinal
638 eccentricity. *Current eye research* 1999, 19, 59-65.
- 639 47. Vorwerk, C.K.; Zurakowski, D.; McDermott, L.M.; Mawrin, C.; Dreyer, E.B. Effects of
640 axonal injury on ganglion cell survival and glutamate homeostasis. *Brain research bulletin*
641 2004, 62, 485-490, doi:10.1016/S0361-9230(03)00075-3.
- 642 48. Lam, T.T.; Siew, E.; Chu, R.; Tso, M.O. Ameliorative effect of MK-801 on retinal ischemia.
643 *Journal of ocular pharmacology and therapeutics : the official journal of the Association for Ocular*
644 *Pharmacology and Therapeutics* 1997, 13, 129-137, doi:10.1089/jop.1997.13.129.
- 645 49. Schuettauf, F.; Naskar, R.; Vorwerk, C.K.; Zurakowski, D.; Dreyer, E.B. Ganglion cell loss
646 after optic nerve crush mediated through AMPA-kainate and NMDA receptors.
647 *Investigative ophthalmology & visual science* 2000, 41, 4313-4316.
- 648 50. Kermer, P.; Klocker, N.; Bahr, M. Modulation of metabotropic glutamate receptors fails to
649 prevent the loss of adult rat retinal ganglion cells following axotomy or N-methyl-D-
650 aspartate lesion in vivo. *Neuroscience letters* 2001, 315, 117-120.
- 651 51. Almasieh, M.; Wilson, A.M.; Morquette, B.; Cueva Vargas, J.L.; Di Polo, A. The molecular
652 basis of retinal ganglion cell death in glaucoma. *Progress in retinal and eye research* 2012, 31,
653 152-181, doi:10.1016/j.preteyeres.2011.11.002.
- 654 52. Manev, H.; Favaron, M.; Guidotti, A.; Costa, E. Delayed increase of Ca²⁺ influx elicited by
655 glutamate: role in neuronal death. *Molecular pharmacology* 1989, 36, 106-112.
- 656 53. Stavrovskaya, I.G.; Kristal, B.S. The powerhouse takes control of the cell: is the
657 mitochondrial permeability transition a viable therapeutic target against neuronal
658 dysfunction and death? *Free radical biology & medicine* 2005, 38, 687-697,
659 doi:10.1016/j.freeradbiomed.2004.11.032.
- 660 54. Hardingham, G.E.; Fukunaga, Y.; Bading, H. Extrasynaptic NMDARs oppose synaptic
661 NMDARs by triggering CREB shut-off and cell death pathways. *Nature neuroscience* 2002, 5,
662 405-414, doi:10.1038/nn835.
- 663 55. Gomez-Vicente, V.; Lax, P.; Fernandez-Sanchez, L.; Rondon, N.; Esquivia, G.; Germain, F.;
664 de la Villa, P.; Cuenca, N. Neuroprotective Effect of Tauroursodeoxycholic Acid on N-
665 Methyl-D-Aspartate-Induced Retinal Ganglion Cell Degeneration. *PloS one* 2015, 10,
666 e0137826, doi:10.1371/journal.pone.0137826.
- 667 56. Wang, S.; Gu, D.; Zhang, P.; Chen, J.; Li, Y.; Xiao, H.; Zhou, G. Melanopsin-expressing
668 retinal ganglion cells are relatively resistant to excitotoxicity induced by N-methyl-d-
669 aspartate. *Neuroscience letters* 2018, 662, 368-373, doi:10.1016/j.neulet.2017.10.055.
- 670 57. Pichavaram, P.; Palani, C.D.; Patel, C.; Xu, Z.; Shosha, E.; Fouda, A.Y.; Caldwell, R.B.;
671 Narayanan, S.P. Targeting Polyamine Oxidase to Prevent Excitotoxicity-Induced Retinal
672 Neurodegeneration. *Frontiers in neuroscience* 2018, 12, 956, doi:10.3389/fnins.2018.00956.
- 673 58. Fahrenthold, B.K.; Fernandes, K.A.; Libby, R.T. Assessment of intrinsic and extrinsic
674 signaling pathway in excitotoxic retinal ganglion cell death. *Scientific reports* 2018, 8, 4641,
675 doi:10.1038/s41598-018-22848-y.
- 676 59. Kobayashi, M.; Hirooka, K.; Ono, A.; Nakano, Y.; Nishiyama, A.; Tsujikawa, A. The
677 Relationship Between the Renin-Angiotensin-Aldosterone System and NMDA Receptor-
678 Mediated Signal and the Prevention of Retinal Ganglion Cell Death. *Investigative*
679 *ophthalmology & visual science* 2017, 58, 1397-1403, doi:10.1167/iovs.16-21001.

- 680 60. Manabe, S.; Gu, Z.; Lipton, S.A. Activation of matrix metalloproteinase-9 via neuronal nitric
681 oxide synthase contributes to NMDA-induced retinal ganglion cell death. *Investigative*
682 *ophthalmology & visual science* **2005**, *46*, 4747-4753, doi:10.1167/iovs.05-0128.
- 683 61. Lambuk, L.; Iezhitsu, I.; Agarwal, R.; Bakar, N.S.; Agarwal, P.; Ismail, N.M. Antiapoptotic
684 effect of taurine against NMDA-induced retinal excitotoxicity in rats. *Neurotoxicology* **2019**,
685 *70*, 62-71, doi:10.1016/j.neuro.2018.10.009.
- 686 62. Tsoka, P.; Barbisan, P.R.; Kataoka, K.; Chen, X.N.; Tian, B.; Bouzika, P.; Miller, J.W.;
687 Paschalis, E.I.; Vavvas, D.G. NLRP3 inflammasome in NMDA-induced retinal
688 excitotoxicity. *Experimental eye research* **2019**, *181*, 136-144, doi:10.1016/j.exer.2019.01.018.
- 689 63. Ito, A.; Tsuda, S.; Kunikata, H.; Toshifumi, A.; Sato, K.; Nakazawa, T. Assessing retinal
690 ganglion cell death and neuroprotective agents using real time imaging. *Brain research* **2019**,
691 *1714*, 65-72, doi:10.1016/j.brainres.2019.02.008.
- 692 64. DeParis, S.; Caprara, C.; Grimm, C. Intrinsically photosensitive retinal ganglion cells are
693 resistant to N-methyl-D-aspartic acid excitotoxicity. *Molecular vision* **2012**, *18*, 2814-2827.
- 694 65. Vidal-Villegas, B.; Miralles de Imperial-Ollero, J.A., Nadal-Nicolás, F.M., Ortín-Martínez,
695 A., Bernal-Garro, J.M., Vidal-Sanz, M., Villegas-Pérez, M.P. Effects of intravitreal injections
696 of N-Methyl-D-Aspartate on melanopsin and non-melanopsin containing retinal ganglion
697 cells in the adult rat. *Ophthalmic Res.* **2017**, *57*,25.
- 698 66. Salinas-Navarro, M.; Mayor-Torroglosa, S.; Jimenez-Lopez, M.; Aviles-Trigueros, M.;
699 Holmes, T.M.; Lund, R.D.; Villegas-Perez, M.P.; Vidal-Sanz, M. A computerized analysis of
700 the entire retinal ganglion cell population and its spatial distribution in adult rats. *Vision*
701 *research* **2009**, *49*, 115-126, doi:10.1016/j.visres.2008.09.029.
- 702 67. Nadal-Nicolas, F.M.; Jimenez-Lopez, M.; Sobrado-Calvo, P.; Nieto-Lopez, L.; Canovas-
703 Martinez, I.; Salinas-Navarro, M.; Vidal-Sanz, M.; Agudo, M. Brn3a as a marker of retinal
704 ganglion cells: qualitative and quantitative time course studies in naive and optic nerve-
705 injured retinas. *Investigative ophthalmology & visual science* **2009**, *50*, 3860-3868,
706 doi:10.1167/iovs.08-3267.
- 707 68. Ortin-Martinez, A.; Jimenez-Lopez, M.; Nadal-Nicolas, F.M.; Salinas-Navarro, M.; Alarcon-
708 Martinez, L.; Sauve, Y.; Villegas-Perez, M.P.; Vidal-Sanz, M.; Agudo-Barriuso, M.
709 Automated quantification and topographical distribution of the whole population of S- and
710 L-cones in adult albino and pigmented rats. *Investigative ophthalmology & visual science* **2010**,
711 *51*, 3171-3183, doi:10.1167/iovs.09-4861.
- 712 69. Nadal-Nicolas, F.M.; Vidal-Sanz, M.; Agudo-Barriuso, M. The aging rat retina: from
713 function to anatomy. *Neurobiology of aging* **2018**, *61*, 146-168,
714 doi:10.1016/j.neurobiolaging.2017.09.021.
- 715 70. Della Santina, L.; Ou, Y. Who's lost first? Susceptibility of retinal ganglion cell types in
716 experimental glaucoma. *Experimental eye research* **2017**, *158*, 43-50,
717 doi:10.1016/j.exer.2016.06.006.
- 718 71. Vidal-Sanz, M.; Galindo-Romero, C.; Valiente-Soriano, F.J.; Nadal-Nicolas, F.M.; Ortin-
719 Martinez, A.; Rovere, G.; Salinas-Navarro, M.; Lucas-Ruiz, F.; Sanchez-Migallon, M.C.;
720 Sobrado-Calvo, P., et al. Shared and Differential Retinal Responses against Optic Nerve
721 Injury and Ocular Hypertension. *Frontiers in neuroscience* **2017**, *11*, 235,
722 doi:10.3389/fnins.2017.00235.
- 723 72. Garcia-Ayuso, D.; Galindo-Romero, C.; Di Pierdomenico, J.; Vidal-Sanz, M.; Agudo-
724 Barriuso, M.; Villegas Perez, M.P. Light-induced retinal degeneration causes a transient
725 downregulation of melanopsin in the rat retina. *Experimental eye research* **2017**, *161*, 10-16,
726 doi:10.1016/j.exer.2017.05.010.
- 727 73. Sanchez-Migallon, M.C.; Valiente-Soriano, F.J.; Nadal-Nicolas, F.M.; Di Pierdomenico, J.;
728 Vidal-Sanz, M.; Agudo-Barriuso, M. Survival of melanopsin expressing retinal ganglion

- 729 cells long term after optic nerve trauma in mice. *Experimental eye research* **2018**, *174*, 93-97,
730 doi:10.1016/j.exer.2018.05.029.
- 731 74. Lax, P., Ortuño-Lizarán, I., Maneu, V., Vidal-Sanz M., Cuenca, N. Melanopsin-containing
732 ganglion cells in the healthy and disease retina. *International Journal of Molecular Sciences*
733 **2019** (Submitted).
- 734 75. Huang, W.; Hu, F.; Wang, M.; Gao, F.; Xu, P.; Xing, C.; Sun, X.; Zhang, S.; Wu, J.
735 Comparative analysis of retinal ganglion cell damage in three glaucomatous rat models.
736 *Experimental eye research* **2018**, *172*, 112-122, doi:10.1016/j.exer.2018.03.019.
- 737 76. Villegas-Perez, M.P.; Vidal-Sanz, M.; Rasminsky, M.; Bray, G.M.; Aguayo, A.J. Rapid and
738 protracted phases of retinal ganglion cell loss follow axotomy in the optic nerve of adult
739 rats. *Journal of neurobiology* **1993**, *24*, 23-36, doi:10.1002/neu.480240103.
- 740 77. Endo, K.; Nakamachi, T.; Seki, T.; Kagami, N.; Wada, Y.; Nakamura, K.; Kishimoto, K.;
741 Hori, M.; Tsuchikawa, D.; Shinntani, N., et al. Neuroprotective effect of PACAP against
742 NMDA-induced retinal damage in the mouse. *Journal of molecular neuroscience : MN* **2011**,
743 *43*, 22-29, doi:10.1007/s12031-010-9434-x.
- 744 78. Lebrun-Julien, F.; Duplan, L.; Pernet, V.; Osswald, I.; Sapieha, P.; Bourgeois, P.; Dickson, K.;
745 Bowie, D.; Barker, P.A.; Di Polo, A. Excitotoxic death of retinal neurons in vivo occurs via a
746 non-cell-autonomous mechanism. *The Journal of neuroscience : the official journal of the Society*
747 *for Neuroscience* **2009**, *29*, 5536-5545, doi:10.1523/JNEUROSCI.0831-09.2009.
- 748 79. Salinas-Navarro, M.; Alarcon-Martinez, L.; Valiente-Soriano, F.J.; Jimenez-Lopez, M.;
749 Mayor-Torroglosa, S.; Aviles-Trigueros, M.; Villegas-Perez, M.P.; Vidal-Sanz, M. Ocular
750 hypertension impairs optic nerve axonal transport leading to progressive retinal ganglion
751 cell degeneration. *Experimental eye research* **2010**, *90*, 168-183, doi:10.1016/j.exer.2009.10.003.
- 752 80. Cuenca, N.; Pinilla, I.; Fernandez-Sanchez, L.; Salinas-Navarro, M.; Alarcon-Martinez, L.;
753 Aviles-Trigueros, M.; de la Villa, P.; Miralles de Imperial, J.; Villegas-Perez, M.P.; Vidal-
754 Sanz, M. Changes in the inner and outer retinal layers after acute increase of the intraocular
755 pressure in adult albino Swiss mice. *Experimental eye research* **2010**, *91*, 273-285,
756 doi:10.1016/j.exer.2010.05.020.
- 757 81. Rovere, G.; Nadal-Nicolas, F.M.; Wang, J.; Bernal-Garro, J.M.; Garcia-Carrillo, N.; Villegas-
758 Perez, M.P.; Agudo-Barriuso, M.; Vidal-Sanz, M. Melanopsin-Containing or Non-
759 Melanopsin-Containing Retinal Ganglion Cells Response to Acute Ocular Hypertension
760 With or Without Brain-Derived Neurotrophic Factor Neuroprotection. *Investigative*
761 *ophthalmology & visual science* **2016**, *57*, 6652-6661, doi:10.1167/iovs.16-20146.
- 762 82. Lam, T.T.; Abler, A.S.; Kwong, J.M.; Tso, M.O. N-methyl-D-aspartate (NMDA)--induced
763 apoptosis in rat retina. *Investigative ophthalmology & visual science* **1999**, *40*, 2391-2397.
- 764 83. Li, Y.; Schlamp, C.L.; Nickells, R.W. Experimental induction of retinal ganglion cell death in
765 adult mice. *Investigative ophthalmology & visual science* **1999**, *40*, 1004-1008.
- 766 84. Akopian, A.; Atlasz, T.; Pan, F.; Wong, S.; Zhang, Y.; Volgyi, B.; Paul, D.L.; Bloomfield, S.A.
767 Gap junction-mediated death of retinal neurons is connexin and insult specific: a potential
768 target for neuroprotection. *The Journal of neuroscience : the official journal of the Society for*
769 *Neuroscience* **2014**, *34*, 10582-10591, doi:10.1523/JNEUROSCI.1912-14.2014.
- 770 85. Siliprandi, R.; Canella, R.; Carmignoto, G.; Schiavo, N.; Zanellato, A.; Zanoni, R.; Vantini, G.
771 N-methyl-D-aspartate-induced neurotoxicity in the adult rat retina. *Visual neuroscience* **1992**,
772 *8*, 567-573.
- 773 86. Volgyi, B.; Chheda, S.; Bloomfield, S.A. Tracer coupling patterns of the ganglion cell
774 subtypes in the mouse retina. *The Journal of comparative neurology* **2009**, *512*, 664-687,
775 doi:10.1002/cne.21912.

- 776 87. Cui, Q.; Ren, C.; Sollars, P.J.; Pickard, G.E.; So, K.F. The injury resistant ability of
777 melanopsin-expressing intrinsically photosensitive retinal ganglion cells. *Neuroscience* **2015**,
778 *284*, 845-853, doi:10.1016/j.neuroscience.2014.11.002.
- 779 88. Valiente-Soriano, F.J.; Nadal-Nicolas, F.M.; Salinas-Navarro, M.; Jimenez-Lopez, M.; Bernal-
780 Garro, J.M.; Villegas-Perez, M.P.; Agudo-Barriuso, M.; Vidal-Sanz, M. BDNF Rescues RGCs
781 But Not Intrinsically Photosensitive RGCs in Ocular Hypertensive Albino Rat Retinas.
782 *Investigative ophthalmology & visual science* **2015**, *56*, 1924-1936, doi:10.1167/iovs.15-16454.
- 783 89. Jakobs, T.C.; Ben, Y.; Masland, R.H. Expression of mRNA for glutamate receptor subunits
784 distinguishes the major classes of retinal neurons, but is less specific for individual cell
785 types. *Molecular vision* **2007**, *13*, 933-948.
- 786 90. Perez de Sevilla Muller, L.; Sargoy, A.; Rodriguez, A.R.; Brecha, N.C. Melanopsin ganglion
787 cells are the most resistant retinal ganglion cell type to axonal injury in the rat retina. *PloS*
788 *one* **2014**, *9*, e93274, doi:10.1371/journal.pone.0093274.
- 789 91. Nadal-Nicolas, F.M.; Sobrado-Calvo, P.; Jimenez-Lopez, M.; Vidal-Sanz, M.; Agudo-
790 Barriuso, M. Long-Term Effect of Optic Nerve Axotomy on the Retinal Ganglion Cell Layer.
791 *Investigative ophthalmology & visual science* **2015**, *56*, 6095-6112, doi:10.1167/iovs.15-17195.
- 792 92. Robinson, G.A.; Madison, R.D. Axotomized mouse retinal ganglion cells containing
793 melanopsin show enhanced survival, but not enhanced axon regrowth into a peripheral
794 nerve graft. *Vision research* **2004**, *44*, 2667-2674, doi:10.1016/j.visres.2004.06.010.
- 795 93. Daniel, S.; Clark, A.F.; McDowell, C.M. Subtype-specific response of retinal ganglion cells
796 to optic nerve crush. *Cell death discovery* **2018**, *4*, 7, doi:10.1038/s41420-018-0069-y.
- 797 94. Vugler, A.A.; Semo, M.; Joseph, A.; Jeffery, G. Survival and remodeling of melanopsin cells
798 during retinal dystrophy. *Visual neuroscience* **2008**, *25*, 125-138,
799 doi:10.1017/S0952523808080309.
- 800 95. Esquivia, G.; Lax, P.; Cuenca, N. Impairment of intrinsically photosensitive retinal ganglion
801 cells associated with late stages of retinal degeneration. *Investigative ophthalmology & visual*
802 *science* **2013**, *54*, 4605-4618, doi:10.1167/iovs.13-12120.
- 803 96. Garcia-Ayuso, D.; Di Pierdomenico, J.; Esquivia, G.; Nadal-Nicolas, F.M.; Pinilla, I.; Cuenca,
804 N.; Vidal-Sanz, M.; Agudo-Barriuso, M.; Villegas-Perez, M.P. Inherited Photoreceptor
805 Degeneration Causes the Death of Melanopsin-Positive Retinal Ganglion Cells and
806 Increases Their Coexpression of Brn3a. *Investigative ophthalmology & visual science* **2015**, *56*,
807 4592-4604, doi:10.1167/iovs.15-16808.
- 808 97. La Morgia, C.; Ross-Cisneros, F.N.; Sadun, A.A.; Hannibal, J.; Munarini, A.; Mantovani, V.;
809 Barboni, P.; Cantalupo, G.; Tozer, K.R.; Sancisi, E., et al. Melanopsin retinal ganglion cells
810 are resistant to neurodegeneration in mitochondrial optic neuropathies. *Brain : a journal of*
811 *neurology* **2010**, *133*, 2426-2438, doi:10.1093/brain/awq155.
- 812 98. Georg, B.; Ghelli, A.; Giordano, C.; Ross-Cisneros, F.N.; Sadun, A.A.; Carelli, V.; Hannibal,
813 J.; La Morgia, C. Melanopsin-expressing retinal ganglion cells are resistant to cell injury, but
814 not always. *Mitochondrion* **2017**, *36*, 77-84, doi:10.1016/j.mito.2017.04.003.
- 815 99. Lax, P.; Esquivia, G.; Esteve-Rudd, J.; Ojalora, B.B.; Madrid, J.A.; Cuenca, N. Circadian
816 dysfunction in a rotenone-induced parkinsonian rodent model. *Chronobiology international*
817 **2012**, *29*, 147-156, doi:10.3109/07420528.2011.649870.
- 818 100. Wulff, K.; Gatti, S.; Wettstein, J.G.; Foster, R.G. Sleep and circadian rhythm disruption in
819 psychiatric and neurodegenerative disease. *Nature reviews. Neuroscience* **2010**, *11*, 589-599,
820 doi:10.1038/nrn2868.
- 821 101. Nadal-Nicolas, F.M.; Madeira, M.H.; Salinas-Navarro, M.; Jimenez-Lopez, M.; Galindo-
822 Romero, C.; Ortin-Martinez, A.; Santiago, A.R.; Vidal-Sanz, M.; Agudo-Barriuso, M.
823 Transient Downregulation of Melanopsin Expression After Retrograde Tracing or Optic

- 824 Nerve Injury in Adult Rats. *Investigative ophthalmology & visual science* 2015, 56, 4309-
825 4323, doi:10.1167/iovs.15-16963.
- 826 102. Semo, M.; Gias, C.; Ahmado, A.; Vugler, A. A role for the ciliary marginal zone in the
827 melanopsin-dependent intrinsic pupillary light reflex. *Experimental eye research* 2014, 119,
828 8-18, doi:10.1016/j.exer.2013.11.013.
- 829 103. Zhang, J.; Diamond, J.S. Subunit- and pathway-specific localization of NMDA receptors
830 and scaffolding proteins at ganglion cell synapses in rat retina. *The Journal of neuroscience*
831 : the official journal of the Society for Neuroscience 2009, 29, 4274-4286,
832 doi:10.1523/JNEUROSCI.5602-08.2009.
- 833 104. Jakobs, T.C.; Libby, R.T.; Ben, Y.; John, S.W.; Masland, R.H. Retinal ganglion cell
834 degeneration is topological but not cell type specific in DBA/2J mice. *The Journal of cell*
835 *biology* 2005, 171, 313-325, doi:10.1083/jcb.200506099.
- 836 105. Li, S.Y.; Yau, S.Y.; Chen, B.Y.; Tay, D.K.; Lee, V.W.; Pu, M.L.; Chan, H.H.; So, K.F. Enhanced
837 survival of melanopsin-expressing retinal ganglion cells after injury is associated with the
838 PI3 K/Akt pathway. *Cellular and molecular neurobiology* 2008, 28, 1095-1107,
839 doi:10.1007/s10571-008-9286-x.
- 840 106. Seki, T.; Nakatani, M.; Taki, C.; Shinohara, Y.; Ozawa, M.; Nishimura, S.; Ito, H.; Shioda, S.
841 Neuroprotective effect of PACAP against kainic acid-induced neurotoxicity in rat retina.
842 *Annals of the New York Academy of Sciences* 2006, 1070, 531-534,
843 doi:10.1196/annals.1317.074.
- 844 107. Nakatani, M.; Seki, T.; Shinohara, Y.; Taki, C.; Nishimura, S.; Takaki, A.; Shioda, S. Pituitary
845 adenylate cyclase-activating peptide (PACAP) stimulates production of interleukin-6 in rat
846 Muller cells. *Peptides* 2006, 27, 1871-1876, doi:10.1016/j.peptides.2005.12.011.
- 847 108. Belenky, M.A.; Smeraski, C.A.; Provencio, I.; Sollars, P.J.; Pickard, G.E. Melanopsin retinal
848 ganglion cells receive bipolar and amacrine cell synapses. *The Journal of comparative*
849 *neurology* 2003, 460, 380-393, doi:10.1002/cne.10652.
- 850 109. Lin, M.S.; Liao, P.Y.; Chen, H.M.; Chang, C.P.; Chen, S.K.; Chern, Y. Degeneration of
851 ipRGCs in Mouse Models of Huntington's Disease Disrupts Non-Image-Forming Behaviors
852 Before Motor Impairment. *The Journal of neuroscience : the official journal of the Society*
853 *for Neuroscience* 2019, 39, 1505-1524, doi:10.1523/JNEUROSCI.0571-18.2018.
- 854 110. Aviles-Trigueros, M.; Sauve, Y.; Lund, R.D.; Vidal-Sanz, M. Selective innervation of
855 retinorecipient brainstem nuclei by retinal ganglion cell axons regenerating through
856 peripheral nerve grafts in adult rats. *The Journal of neuroscience : the official journal of the*
857 *Society for Neuroscience* 2000, 20, 361-374.
- 858 111. Lindqvist, N.; Peinado-Ramonn, P.; Vidal-Sanz, M.; Hallbook, F. GDNF, Ret, GFRalpha
859 and 2 in the adult rat retino-tectal system after optic nerve transection. *Experimental*
860 *neurology* 2004, 187, 487-499, doi:10.1016/j.expneurol.2004.02.002.
- 861 112. Di Pierdomenico, J.; Garcia-Ayuso, D.; Jimenez-Lopez, M.; Agudo-Barriuso, M.; Vidal-Sanz,
862 M.; Villegas-Perez, M.P. Different Ipsi- and Contralateral Glial Responses to Anti-VEGF
863 and Triamcinolone Intravitreal Injections in Rats. *Investigative ophthalmology & visual*
864 *science* 2016, 57, 3533-3544, doi:10.1167/iovs.16-19618.
- 865 113. Rovere, G.; Nadal-Nicolas, F.M.; Agudo-Barriuso, M.; Sobrado-Calvo, P.; Nieto-Lopez, L.;
866 Nucci, C.; Villegas-Perez, M.P.; Vidal-Sanz, M. Comparison of Retinal Nerve Fiber Layer
867 Thinning and Retinal Ganglion Cell Loss After Optic Nerve Transection in Adult Albino
868 Rats. *Investigative ophthalmology & visual science* 2015, 56, 4487-4498, doi:10.1167/iovs.15-
869 17145.
- 870 114. Ortin-Martinez, A.; Salinas-Navarro, M.; Nadal-Nicolas, F.M.; Jimenez-Lopez, M.; Valiente-
871 Soriano, F.J.; Garcia-Ayuso, D.; Bernal-Garro, J.M.; Aviles-Trigueros, M.; Agudo-Barriuso,
872 M.; Villegas-Perez, M.P., et al. Laser-induced ocular hypertension in adult rats does not

- 873 affect non-RGC neurons in the ganglion cell layer but results in protracted severe loss of
874 cone-photoreceptors. *Experimental eye research* 2015, 132, 17-33,
875 doi:10.1016/j.exer.2015.01.006.
- 876 115. Sanchez-Migallon, M.C.; Valiente-Soriano, F.J.; Nadal-Nicolas, F.M.; Vidal-Sanz, M.;
877 Agudo-Barriuso, M. Apoptotic Retinal Ganglion Cell Death After Optic Nerve Transection
878 or Crush in Mice: Delayed RGC Loss With BDNF or a Caspase 3 Inhibitor. *Investigative*
879 *ophthalmology & visual science* 2016, 57, 81-93, doi:10.1167/iovs.15-17841.
- 880 116. Vidal-Sanz, M.; Salinas-Navarro, M.; Nadal-Nicolas, F.M.; Alarcon-Martinez, L.; Valiente-
881 Soriano, F.J.; de Imperial, J.M.; Aviles-Trigueros, M.; Agudo-Barriuso, M.; Villegas-Perez,
882 M.P. Understanding glaucomatous damage: anatomical and functional data from ocular
883 hypertensive rodent retinas. *Progress in retinal and eye research* 2012, 31, 1-27,
884 doi:10.1016/j.preteyeres.2011.08.001.
- 885 117. Vidal-Sanz, M.; Valiente-Soriano, F.J.; Ortin-Martinez, A.; Nadal-Nicolas, F.M.; Jimenez-
886 Lopez, M.; Salinas-Navarro, M.; Alarcon-Martinez, L.; Garcia-Ayuso, D.; Aviles-Trigueros,
887 M.; Agudo-Barriuso, M., et al. Retinal neurodegeneration in experimental glaucoma.
888 *Progress in brain research* 2015, 220, 1-35, doi:10.1016/bs.pbr.2015.04.008.

889